Breathing Rate Estimation & Apnea Detection with Multiple Elevated and Tilted FMCW Radars

Wendelmuth, M.; Yarovoy, A.; Fioranelli, F.

DOI
10.1109/RadarConf2559087.2025.11205082

Publication date
2025

Document Version
Final published version

Published in
Proceedings of the 2025 IEEE Radar Conference, RadarConf 2025

Breathing rate estimation & apnea detection with multiple elevated and tilted FMCW radars

Mareike Wendelmuth, Alexander Yarovoy, Francesco Fioranelli
Microwave Sensing, Signals & Systems (MS3) Group
Delft University of Technology
Delft, Netherlands
(m.wendelmuth, a.yarovoy, f.fioranelli)@tudelft.nl

2025 IEEE Radar Conference (RadarConf25) | 979-8-3315-4433-1/25/$31.00 ©2025 IEEE | DOI: 10.1109/RADARCONF2559087.2025.11205082

***Abstract*—The problem of estimating breathing rates and detecting apnea events with radars located at an elevated and tilted position is considered in this paper. This is particularly relevant in psychiatric clinics, where radars (or other sensors) must be installed out of reach of patients. In this work, a feasibility study is presented, using an experimental setup with two 60 GHz Frequency-Modulated Continuous Wave (FMCW) radars placed at 2.7 m height at a tilted angle towards the participants, and one radar at 1 m height looking straight to the participants, who are sitting and lying on the floor. A new comprehensive dataset with 30 participants and 7 activities was collected with this setup. Using phase extraction and filtering, the work presents an apnea detection probability of up to 90 % with an elevated radar, and comparable mean error rates for breathing estimation of below 2 respirations per minute (rpm) for all radars. The results show that the respiration data and apnea detection from all radar positions are comparable. This proves the feasibility of the proposed radar deployment positions, benefiting application fields such as psychiatric care.**

***Index Terms*—Vital signs monitoring, MIMO radars, mmWave radar**

I. Introduction

Monitoring human vital signs such as heart rate, respiration rate, blood pressure, and temperature is necessary and beneficial in clinical settings. Measuring and gathering them has been defined as the 'simplest, cheapest and probably the most important' aspect for clinical observation and early warning systems [1]. While most conventional monitoring approaches are based on wearables, like belts and watches, electrocardiograms (ECG), and photoplethysmography (PPG), the application of radar systems in healthcare has gained more popularity over the last few years. Radars benefit from contactless monitoring without ambient light dependencies, allowing advanced human monitoring. The possibility of embedding radar in a home environment while causing limited privacy infringement makes it a promising technology for the future to automate monitoring of vital signs and activity patterns [2]–[4]. Moreover, the lack of medical personnel and the increasing age of the population are leading to the necessity of new, automatic methods for patient observation. Radar applications in elderly homes, smart homes, and cars have been the topic of last year's research [5], while hospitals and specifically psychiatric clinics still lag relatively behind these new developments. With a decrease in available trained staff and new insights into treatment methods, new observation technologies are the next necessary step for better overall care.

Focusing on psychiatric clinics, seclusion rooms are still frequently used by volatile patients and lack continuous observation possibilities for healthcare personnel. Patients are usually placed in those rooms when endangered to hurt themself or the surrounding people. To avoid dangerous situations, the interior of these rooms is usually limited to a mattress and sometimes a toilet. Any patient observation has to be done manually by personnel or from a distance, with devices out of reach for the patients. While current observation with cameras allows no detection of vital signs, these are key parameters to detect the state of a person. Radar would allow vital sign estimation and human activity recognition without physical contact. To the best of our knowledge, the application of radar in seclusion rooms, and even psychiatric clinics, to measure vital signs and classify dangerous and safe situations has not been investigated. For application in the psychiatric clinics, the radars must be out of reach, placed high, close to, or at the ceiling. They will have a tilted placement towards the person to cover the whole room. New approaches must be tested and compared to the current state of the art, which uses primarily frontal, chest-facing, short-distance observation [6]–[9]. However, this introduces new challenges: stronger clutter from the floor, the unusual perspective with changes of azimuth elevation and ranges, and guaranteeing coverage while minimizing the number of radars are all topics to address with this placement. To the best of our knowledge, this tilted placement has only been limitedly investigated for human activity recognition (HAR) [10].

Impulse Radio Ultra-Wideband (IR-UWB) [6], [11] and Frequency-Modulated Continuous Wave (FMCW) [3], [12] radars have been used to estimate breathing rates of static and non-static persons from a close distance. Most of the time, the radar was placed at chest height and close to the patient, or above a bed facing the patient, with only a few exceptions of elevated radar positions for vital sign estimation [13]. The capability of measuring patients with devices out of their reach, allowing vital sign recognition from more than 5 m away, which is crucial in psychiatry, has not been well investigated to the best of our knowledge.

This work investigates the possibilities of an elevated and tilted FMCW radar placement. It compares the results to the

standard positioning, placing two radars at ceiling height and one at hip-height for reference. A dataset consisting of 30 participants and 7 activities has been collected. Using phase extraction and filtering, the detection of apnea events and estimation of breathing rate, which play an essential role in suicide prevention for clinics and medical centres, was shown to be feasible with these new radar positions.

The rest of the paper is organised as follows. In section II, the proposed processing pipeline is presented. Then, section III gives some insights into the collected dataset for this work, and section IV presents the comparison results between the elevated radars and the hip-height placed radar, proving the feasibility of the proposed approaches. Finally, section V concludes this paper and gives some outlook to future work.

II. Proposed Processing

Conventionally, human vital signs are modelled with two sinusoidal signals with different amplitudes and frequencies for respiration and heart rate, respectively. The resulting displacement $\Delta R(t)$ of the chest, measured by the radar, can be modelled as:

$$\Delta R(t) \equiv \delta_b(t) + \delta_h(t) \tag{1}$$

where $\delta_b(t)$ and $\delta_h(t)$ are the chest displacements due to the breath and heart rate, respectively. Further derivation of the displacement signals for FMCW radars is found in [3] and used as an inspiration for the subsequent processing.

The raw I/Q data measured by the three FMCW radars used in this work are processed individually to compare the results of each radar with respect to its deployment position. The first processing steps are similar for the apnea detection and the breathing rate estimation task, as shown in Figure 1. It should be noted that for the breathing rate estimation, the raw data during the time of apnea episodes was removed from the radar and reference data.

Firstly, the localization of the response from a human chest is done via 2D Fast Fourier Transform (FFT) of the measured signals over fast and slow time, with zero padding to 256 and 512 samples, respectively, and detection in the Range-Doppler plane. Secondly, for the selected range bin with maximum power, Multiple-input-Multiple-output (MIMO) digital beamforming in azimuth and elevation is performed on the range profile data, and the angular cell with the largest signal-to-noise ratio (SNR) is selected. This range-angular cell position is assumed to be constant for a period of 20 seconds to perform phase extraction. Thirdly, for that particular cell, a coherent summation over 10 consecutive chirps (i.e., around 1.34 ms) and 5 neighbouring range bins (i.e., around 0.19 m) to cover the whole body area is performed prior to the extraction of the phase information $\phi(t)$ as follows:

$$\phi(t) = \text{unwrap}\left[\tan^{-1}\left(\frac{Q(t)}{I(t)}\right)\right] \tag{2}$$

where $Q(t)$ and $I(t)$ are the real and imaginary parts of the summed signal of multiple chirps and range bins with digital beamforming.

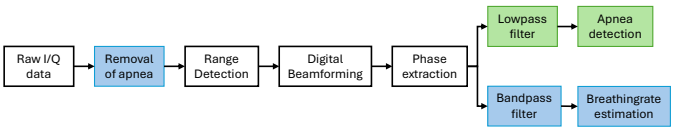

Fig. 1. Flowchart describing the signal processing steps for apnea detection and breathing rate estimation. The white steps are followed for both processing schemes, while the green or blue are only followed for apnea detection or breathing rate detection, respectively.

A. Apnea detection

To detect apnea events, the phase signal $\phi(t)$ was lowpass filtered with a cut-off frequency of 0.5 Hz to remove unwanted faster components. During the apnea, the changes in the phase signal decreased due to smaller changes in the chest. This effect is easier to see by computing the derivative of the phase signal. This represents the velocity change of the chest, enabling to detect the apnea more easily, as its velocity is close to zero. A threshold on the resulting gradient signal was thus used to detect the apnea. Different threshold settings were tried in this work: mean, median of the signal, or 24 % of the signal's maximum. If this threshold was not passed for at least 5 seconds, the corresponding data section was counted as an apnea event. Figure 2 shows examples of the signals and the detected apnea for one participant and one radar.

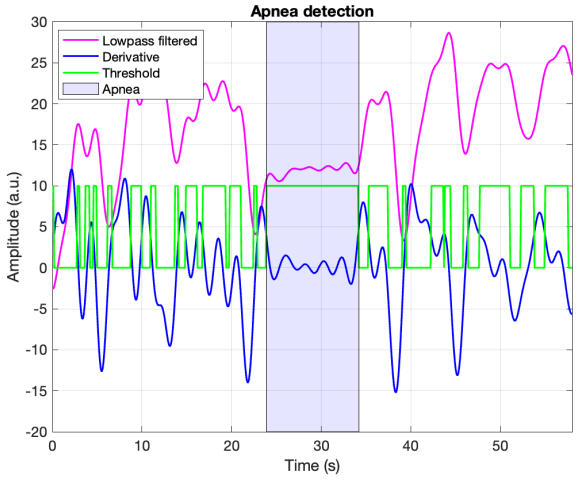

Fig. 2. Example of signals for apnea detection. In magenta is the lowpass filtered signal, and in blue its derivative. Using the proposed threshold based on the mean of the derivative, the green signal is used to detect the marked apnea (segment in light blue shade).

B. Breathing rate estimation

The breathing rate from the radar signal and the respiration belt's reference signal were calculated after removing the apnea events and the previously described processing steps. The phase signal was filtered with a bandpass filter in the range $[0.1, 0.5]$ Hz [11], [12]. This corresponds to a breathing rate of 6 to 30 rpm, which aligns with the breathing rates from the reference respiration belt. The respiration rate was then

estimated using the Short-Time Fourier Transform (STFT) with a Hann window of 20 s and an overlap length of 75%. The belt's respiration rate was determined similarly: after bandpass filtering, STFT was applied. An example of radar and respiration belt signals for one participant is shown in Figure 3. The gap represents the removed apnea event.

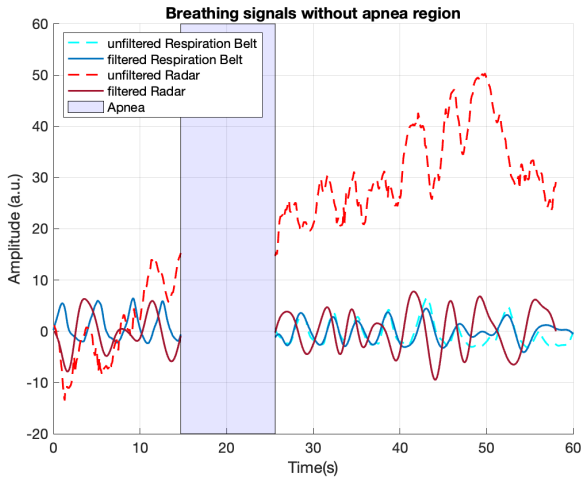

Fig. 3. Examples of breathing signals from respiration belt (blue shades) and radar (red shades), before (dashed line) and after bandpass filtering (constant line). The gap represents a portion of the signal with an apnea event that has been removed.

III. Dataset

The dataset used for this work was recorded in February 2025 and consists of 30 voluntary participants performing seven activities of one minute each. 23 male and 7 female participants were recorded. The mean age was 30.6 years with a standard deviation (STD) of 7.5 years, and the average height was 178.1 cm with a STD of 6.7 cm[1]. The data collection was approved by the TU Delft HREC Committee, and each participant was informed about it accordingly and signed a consent form.

A. Experimental Setup

The experimental setup included three combinations of the IWR6843ISK [15] radar board and the DCA1000EVM evaluation board from Texas Instruments (TI). Two radar units were mounted close to the ceiling (2.7 m from the floor) at a tilted angle to illuminate a common area in the room, and one unit was mounted at hip height (approximately 1 m from the floor). The naming of the three radars follows a clockwise order and starts with Radar 1 at the top left corner. The setup is shown in Figure 4, including a closer view of the tilted Radar 2. All three radar boards were operated in frequency division multiple access (FDMA) mode at starting frequencies of 60, 61.25, and 62.5 GHz, respectively, with a bandwidth of 1 GHz. This was done to avoid potential mutual interference

[1]Note that only 28 of the 30 participants provided height and age information.

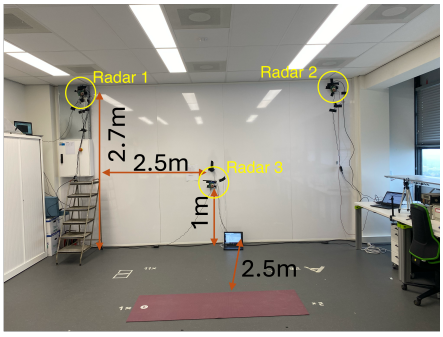

(a) Mounted radars.

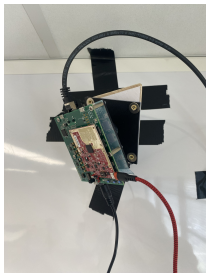

(b) Zoom on tilted Radar 2 unit.

Fig. 4. Picture of the setup with three radars. Radar 1 and Radar 2 were placed close to the ceiling in a tiled and rotated position, and Radar 3 was located at hip height without any rotation for reference. The mattress at the centre is used for the vital sign measurements.

TABLE I
Chosen parameters for the TI IWR6843ISK radar boards [15] for the dataset collection to record both HAR and detect vital signs.

Parameters	Symbol	Value
Start freq		60, 61.25, 62.5 GHz
Ramp End time	T_{ramp}	44 μs
Frequency slope	S	25 MHz/μs
ADC samples		80
Sample Rate	f_s	2000 ksps
Bandwidth	B	1 GHz
Chirps per Frame		120
Frame periodicity		100 ms
Active TX/RX		3/4
Maximum range	R_{max}	11.99 m
Range resolution	ΔR	0.15 m
Maximum velocity	v_{max}	3.1 m/s
Velocity resolution	Δv	0.15 m/s

due to overlapping operating bands. The exact parameters of the radar units are given in Table I.

As ground truth for respiration measurements, the Vernier Go Direct [16] respiration belt was used. It uses a force sensor and a nylon strap around the chest. At rest, this allows straightforward measurements of the breathing rate. The alignment of the radar and the respiration belt data for comparison was done manually.

B. Activities

The choice of activities to be recorded was based on insights from collaborators in the Psychiatry Department of the Erasmus Medical Centre, Rotterdam, and other collaborators in mental health organizations. Each participant was asked to perform seven activities. Three of these focused on vital sign detection, and four on activity recognition. Each activity was overall 1 minute long. For each activity, the ground truth of the respiration belt was also recorded[2]. Activity #6 and #7

[2]It has to be noted that for the activities that include movements, the respiration belt data is mostly not clear enough to recognize the breathing rhythm.

were split into two sequences of 30 seconds while recording, allowing two different positions and a short rest of 10 seconds in between. For this work, only the activities *Sitting* and *Lying on the back* were considered and explained in more detail in the following. The seven activities were:

1) **Sitting**: The participant had to sit on the mattress facing the wall, breathing normally. During the recording of 1 minute, the participant was asked to hold their breath at some point for some seconds to simulate an instance of apnea[3]. In all recorded cases, breathing is detectable in the respiration belt data.
2) **Lying on the back**: The participant lay on their back facing the ceiling and breathed normally (i.e., supine position). During the recording of 1 minute, the participant was asked to hold their breath at some point for some seconds to simulate an instance of apnea[3] . Even in these cases, the breathing is detectable in the data of the respiration belt.
3) Lying on the side
4) Turning / Restless movement while lying
5) Walking
6) Jumping Jacks
7) Boxing / Kicking

For all participants, all activities were recorded once with all three radars at the same time. This led to 210 minutes of total records for each radar. Due to some malfunctioning of the radars, some recordings had to be repeated to achieve a simultaneous measurement of all three radars. The faulty recordings, with only one or two radar recordings out of three, were still saved and can be used later to check interferences, train a classifier, and perform other tasks. Considering also these data, an overall dataset duration of 359 minutes of recorded activities was achieved.

Different activities of the same dataset were used for 3D recognition of extended target signatures in the paper from Lou et al. [14].

IV. Results

In the context of psychiatric clinics, detecting the breathing rate, apnea and stopping of breathing events of patients plays an important role for their well-being and monitoring conditions. However, in this context, the placement of the radars will be only possible at ceiling height to prevent intrusion into the patients and potential damage by them, making the comparison between the different radar positions an essential factor in evaluating the feasibility of this application. Although previous works showed promising results for closely placed radars in front of the chest [8], [12], [17], [18], no radar placement at this offset with a tilted angle and a distance of more than 5 m has been performed in the open literature, to the best of our knowledge. Therefore, this work emphasizes the performance comparison of different positions of the radars, focusing on the feasibility of elevated placements with tilted beams.

[3]Note that 2 out of 30 recordings do not include an apnea event.

A. Apnea detection

An apnea event means that the person's chest is not moving, which is detectable by radar. In the dataset, the participants held their breath for random durations to simulate an apnea. However, further involuntary small chest movements were visible at the same time, making the detection harder. Following the processing steps described in section II, the detected apnea amount per participant was counted and compared to the number of actual apnea events measured with the respiration belt used as a reference. The different thresholds on the derivative of the phase considered in this work were: mean value (100 % and 90 %), median value (100 %) and 24 % of the signal's maximum value. The results are shown in Table II. More specifically, the probability of detection (P_D) is defined as:

$$P_D = \frac{\sum_{i=1}^{30} [\text{Number of apnea}_i \leq \text{Number of detections}_i]}{30} \tag{3}$$

and the number of false alarms (N_{FA}) is the amount of additional detected apneas over all participants:

$$N_{FA} = \frac{\sum_{i=1}^{30} [\text{Number of detections}_i - \text{Number of apneas}_i]}{30} \tag{4}$$

Overall, using the 100 % mean as a threshold showed the best results for the probability of detecting an apnea event. However, this also included a lot of false alarms, which, overall, smaller involuntary chest movements could cause. Decreasing the threshold to 90 % reduced the number of false alarms a lot but also showed less detection probability. Radar 2 provided the best detection probability of 90 % and 83.33 % for the mean-based thresholds. Although Radar 3 was positioned at the lowest position and closest to the participant with a direct view of the chest, the detection probability of apnea was the worst when using the mean- and the max-based threshold.

While the measured apnea events were between 4.6 and 17.3 seconds in duration for the sitting position, in real applications they are most likely of interest only if longer. This would probably increase the detection probability and could reduce the number of false alarms. However, the simple processing approach used in this work detected sufficient apnea events, focusing on minimizing missed detections. The results validate the feasibility of placing the radars at ceiling height with a tilted angle towards the participant. Both Radar 1 and Radar 2 performed similarly to the lower-placed Radar 3. Further investigation into more advanced processing methods and thresholds might improve the detection probabilities and contextually lower the false alarms.

B. Breathing rate estimation

The processing steps previously described in section II were used to estimate the breathing rate for each participant. With the window length of 20 s, an overlap of 75 %, and different removed apnea lengths, 5 to 8 breathing estimations per participant's recording were done. Notably, the breathing rate between the participants varied a lot between 7.03 and

TABLE II
PROBABILITY OF DETECTION (P_D) AND NUMBER OF FALSE ALARMS (N_{FA}) FOR APNEA DETECTION WITH DIFFERENT THRESHOLDS ON THE DERIVATIVE OF THE PHASE, AND ALL THREE RADARS.

		Radar 1	Radar 2	Radar 3
24% Maximum	P_D	83.33 %	86.67 %	70 %
	N_{FA}	0.9	0.867	0.3
100% Median	P_D	66.67 %	73.33 %	73.33 %
	N_{FA}	0.13	0.267	0.267
100% Mean	P_D	86.67 %	90 %	80 %
	N_{FA}	0.46	0.73	0.46
90% Mean	P_D	70 %	83.33 %	70 %
	N_{FA}	0.267	0.367	0.3

22.85 rpm. The ground truth data from the respiration belt was subtracted from each estimation point to compute the error in breathing rate estimation. Afterwards, the mean error for each participant and each radar was calculated. The results of this averaging are shown in Figure 5 for participants sitting on the mattress.

While the mean error often stayed between ± 2 rpm, some outliers up to -10 rpm were recognized. It has to be noted that for some participants, the data without apnea was less than 40 seconds. With the short window of 20 seconds, a difference of 4 rpm might lead to only one additional peak recognized from the STFT output. Moreover, cutting apnea events before performing breathing rate estimation led to additional peaks in the radar data. For better breathing rate estimation, longer windows and no apnea-cutting will be needed. The outliers were also further investigated, and it was found that the breathing could be better recognized by summing up more range bins together, as these participants occupied more range bins than other participants. These initial results show clearly that the different body structures, as well as different breathing ways and rates, make it impossible to use a 'one-fits-all' processing solution. Thus, it is expected that including further processing steps to estimate the precise amount of occupied range bins over time might improve the results.

However, these initial results already show that a breathing rate estimation with an error below 4 rpm was possible for most participants. Moreover, this validated the usage of elevated, tilted radars, as most of the time Radar 1 and Radar 2 performed similarly well as Radar 3. Combining their results with suitable fusion strategies would allow further improved results, possibly outperforming one radar at hip height.

To further validate the results, a second position of the participants was evaluated with the same processing pipeline. The participants were lying on their backs on the mattress, parallel to the wall, with a breathing rate between 5.8 and 25.2 rpm across all participants. Due to high reflections of the ground and the multipath occurring, the results shown in Figure 6 are worse than those of the sitting position. However, for most participants, a valid breathing rate estimation with an error smaller than 4 rpm was possible. It has to be noted that

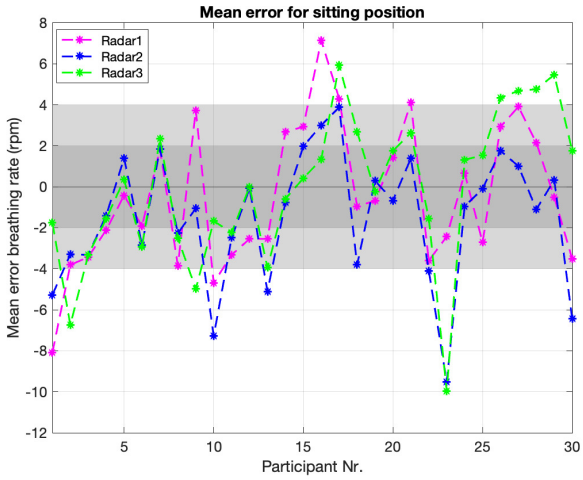

Fig. 5. Mean breathing error rate for each radar compared to the respiration belt for all 30 participants. These results are for the sitting position.

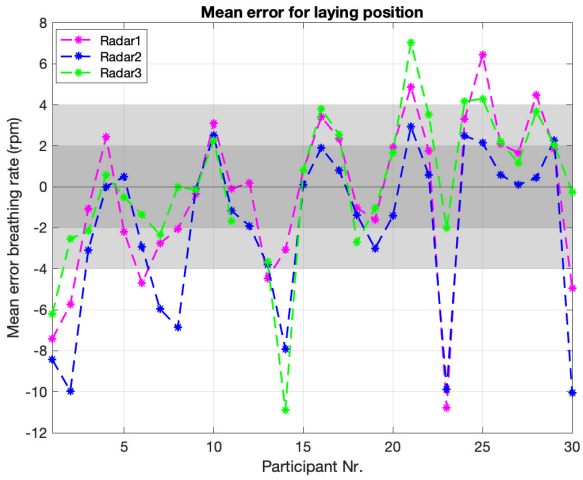

Fig. 6. Mean breathing error rate for each radar compared to the respiration belt for all 30 participants. These results are for the lying on the back position.

the outlier participants #2 and #23 from the sitting position were outliers for the lying position as well, encouraging the need for a different processing to adjust to their breathing pattern and body structure. Furthermore, all radars performed similarly well, showing the feasibility of an elevated radar placement for multiple positions that is very suitable in the context of psychiatry clinics.

To summarise, the overall results of all radar and both participant positions are summarised in Table III, Table IV, and Table V. Although Radar 3 outperforms the elevated radars, the overall results of Radar 1 are very close and show the feasibility of an elevated position. Furthermore, the processing shows for 83 % of the participants mean error of less than 4 rpm for Radar 1. This encourages future work to use elevated and tilted radar positions.

TABLE III
MEAN ERROR AND STANDARD DEVIATION (STD) FOR EACH RADAR, FOR PARTICIPANTS IN THE SITTING AND LYING ON THE BACK POSITIONS.

	Sitting		Laying	
	Mean error	**STD error**	**Mean error**	**STD error**
Radar 1	-0.4431	6.8117	-0.485	7.77426
Radar 2	-1.4984	6.2194	-2.0761	6.6929
Radar 3	-0.1352	6.6555	-0.1025	7.4451

TABLE IV
NUMBER OF PARTICIPANTS WITH A BREATHING RATE ESTIMATION ERROR BELOW 4 RPM AND 2 RPM FOR EACH RADAR AND SITTING POSITION.

	Sitting	
	Mean error $< \pm 4$ rpm	**Mean error $< \pm 2$ rpm**
Radar 1	25	8
Radar 2	24	16
Radar 3	22	14

TABLE V
NUMBER OF PARTICIPANTS WITH A BREATHING RATE ESTIMATION ERROR BELOW 4 RPM AND 2 RPM FOR EACH RADAR AND LYING ON THE BACK POSITION.

	Lying on the back	
	Mean error $< \pm 4$ rpm	**Mean error $< \pm 2$ rpm**
Radar 1	21	11
Radar 2	23	14
Radar 3	24	11

V. CONCLUSION

This paper has considered estimating breathing rate and detecting apnea events with radars located at elevated and tilted positions. A feasibility study with 3 radars (2 mounted on the ceiling and 1 at hip-height) and 30 participants performing seven different activities has been conducted.

The presented results show that apnea detection was possible with the elevated radars, which achieved a detection probability of up to 90 %. The respiration rate estimation was possible with all radars, and the results do not seem to depend directly on the position of the radar. Although the hip-height radar achieved a smaller error using data from a respiration belt as ground truth, both elevated radars performed well and achieved a mean error below 2 rpm. This proves the feasibility of elevated radars for vital signs monitoring in contexts such as psychiatric clinics, where such deployment choice (i.e., radars or sensors on the ceiling, out of the way of patients) is required. Further investigation and improvement in the signal processing for vital signs estimation and classification of the other activities will be conducted in future work.

ACKNOWLEDGMENT

The authors thank Dr Nina Grootendorst from Erasmus Medical Centre and Prof Remco de Winter from GGZ Rivierduinen, who helped us with valuable psychiatric insights and inputs, and all the participants to the data collection. This work was partly supported by the Dutch Research Council NWO with their Impact Explorer grant.

REFERENCES

[1] J. Kellett and F. Sebat, "Make vital signs great again – A call for action," European Journal of Internal Medicine, vol. 45, pp. 13–19, Nov. 2017, doi: 10.1016/j.ejim.2017.09.018.

[2] S. K. Koul and R. Bharadwaj, "UWB and 60 GHz Radar Technology for Vital Sign Monitoring, Activity Classification and Detection," in Wearable Antennas and Body Centric Communication, vol. 787, in Lecture Notes in Electrical Engineering, vol. 787. , Singapore: Springer Singapore, 2021, pp. 219–252. doi: 10.1007/978-981-16-3973-9_8.

[3] G. Paterniani et al., "Radar-Based Monitoring of Vital Signs: A Tutorial Overview," Proc. IEEE, vol. 111, no. 3, pp. 277–317, Mar. 2023, doi: 10.1109/JPROC.2023.3244362.

[4] F. Fioranelli and J. Le Kernec, "Radar sensing for human healthcare: challenges and results," in 2021 IEEE Sensors, Sydney, Australia: IEEE, Oct. 2021, pp. 1–4. doi: 10.1109/SENSORS47087.2021.9639702.

[5] F. Fioranelli, Guendel, Ronny G., Kruse, Nicolas C., and Yarovoy, Alexander, "Radar Sensing in Healthcare: Challenges and Achievements in Human Activity Classification & Vital Signs Monitoring," in Bioinformatics and Biomedical Engineering, Rojas, Ignacio, Valenzuela, Olga, Rojas Ruiz, Fernando, Herrera, Luis Javier, and Ortuno, Francisco, Eds., Springer Nature Switzerland, 2023, pp. 492–504.

[6] M. Mercuri et al., "Enabling Robust Radar-Based Localization and Vital Signs Monitoring in Multipath Propagation Environments," IEEE Trans. Biomed. Eng., vol. 68, no. 11, pp. 3228–3240, Nov. 2021, doi: 10.1109/TBME.2021.3066876.

[7] S. Hazra et al., "Robust Radar-Based Vital Sensing With Adaptive Sinc Filtering and Random Body Motion Rejections," IEEE Sens. Lett., vol. 7, no. 5, pp. 1–4, May 2023, doi: 10.1109/LSENS.2023.3266237.

[8] S. Marty, A. Ronco, F. Pantanella, K. Dheman, and M. Magno, "Frequency Matters: Comparative Analysis of Low-Power FMCW Radars for Vital Sign Monitoring," IEEE Trans. Instrum. Meas., vol. 73, pp. 1–10, 2024, doi: 10.1109/TIM.2024.3381692.

[9] E. Sadeghi, K. Skurule, A. Chiumento, and P. Havinga, "Comprehensive mm-Wave FMCW Radar Dataset for Vital Sign Monitoring: Embracing Extreme Physiological Scenarios," May 21, 2024, arXiv: arXiv:2405.12659. Accessed: Jun. 19, 2024. [Online]. Available: http://arxiv.org/abs/2405.12659

[10] S. Scholes, A. Ruget, Zhu, and J. Leach, "Human pose inference using an elevated mmWave FMCW radar," 2024.

[11] J. Kim and S. Kim, "Proposed Signal Processing Method for Continuous Respiration Monitoring using UWB Radar," in 2024 IEEE International Conference on Consumer Electronics (ICCE), Las Vegas, NV, USA: IEEE, Jan. 2024, pp. 1–4. doi: 10.1109/ICCE59016.2024.10444481.

[12] P. Mehrjouseresht, R. E. Hail, P. Karsmakers, and D. M. M.-P. Schreurs, "Respiration and Heart Rate Monitoring in Smart Homes: An Angular-Free Approach with an FMCW Radar," Sensors, vol. 24, no. 8, p. 2448, Apr. 2024, doi: 10.3390/s24082448.

[13] C. Song, A. D. Droitcour, S. M. M. Islam, A. Whitworth, V. M. Lubecke, and O. Boric-Lubecke, "Unobtrusive occupancy and vital signs sensing for human building interactive systems," Sci Rep, vol. 13, no. 1, p. 954, Jan. 2023, doi: 10.1038/s41598-023-27425-6.

[14] K. Lou, M. Wendelmuth, N. C. Kruse, A. Yarovoy, and F. Fioranelli, "3D Reconstruction of Extended Target Signature with Distributed MIMO Radar Nodes," in IEEE Radar Conference 2025, Krakow, Poland, 2025, submitted.

[15] TI IWR6843ISK, Last viewed 2025-02-26. [Online]. Available: https://www.ti. com/tool/IWR6843ISK

[16] Vernier Go Direct Respiration Belt, Last viewed 2025-02-26. [Online]. Available: https://www.vernier.com/product/go-direct-respiration-belt/

[17] M. Forouzanfar, M. Mabrouk, S. Rajan, M. Bolic, H. R. Dajani, and V. Z. Groza, "Event Recognition for Contactless Activity Monitoring Using Phase-Modulated Continuous Wave Radar," IEEE Trans. Biomed. Eng., vol. 64, no. 2, pp. 479–491, Feb. 2017, doi: 10.1109/TBME.2016.2566619.

[18] D. Wang, S. Yoo, and S. H. Cho, "Experimental Comparison of IR-UWB Radar and FMCW Radar for Vital Signs," Sensors, vol. 20, no. 22, p. 6695, Nov. 2020, doi: 10.3390/s20226695.